

Supporting information for:  
**Water as a reactant in the first step of triosephosphate isomerase catalysis**

**<sup>a</sup>Max Yates and <sup>a</sup>Patrik R. Callis**

*<sup>a</sup> Department of Chemistry and Biochemistry, Montana State University,*

*<sup>a</sup> Bozeman, MT 59717*

Contents

Materials and Methods .....	1
Causes of distance fluctuations seen in Fig. 1(A) of text.....	2
Causes of distance fluctuations seen in Fig. 2(A) of text.....	2
Causes of distance fluctuations seen in Fig. 2(B) of text.....	2
Further discussion of pKa in the enzyme.....	2
Figure S1. ....	2
Figure S2. ....	3
Figure S3. . . . .	3
Figure S4. . . . .	4
Figure S5. . . . .	4
Movie S1. . . . .	5
Movie S2. . . . .	5
References .....	5

**Materials and Methods**

Quantum MD used the method called Atom-centered Density Matrix Propagation method provided by Gaussian09[1] using the keyword ADMP.[2,3] This method describes quantum zero-point and tunneling effects, unlike classical MD, and is stated to provide results equivalent to those from Car-Paranello [4].

Gaussian basis functions instead of primarily plane waves. Energy optimizations were also carried out with Gaussian09, with HF/3-21, b3lyp/6-31g(d,p), and b3lyp/cc-pVTZ.

Classical molecular dynamics were performed with Gromacs version 2016.3 [5] using the SDSC Comet resources. The initial model of the reactant bound state was taken from a high-resolution structure of TIM generated from x-ray crystallography (RCSB PDB, 1NEY) [6]. The inhibitor molecule was modified to the substrate DHAP, which had been manually added to the topology database. The structure was solvated in a box with a volume of 772.11 nm<sup>3</sup> using the SPC/E water model. Simulations used periodic boundary conditions and achieved energy minimization through the steepest descent algorithm. The Amber ff99SB -ILDN force field [7] was used in all simulations, which was performed independently for 10, 50, and 200 nanoseconds.

Electric field calculations employed a homegrown Fortran77 procedure that independently very closely duplicated results published by Skinner and co-workers.[8,9] The input for the program are files in PDB format extracted from the .xtc MD trajectory files generated using Gromacs as noted above.

**Causes of distance fluctuations seen in Fig. 1(A) of text.** During the early 15 ns of the simulation, there is little close water, which is a period during which Ser96 is not yet in contact with Glu165 and water is essentially excluded. Thereafter, however, ~10-15 ns-periods of uninterrupted water trapped near the proton to be abstracted are common. The large transient distance increases from OE1 and OE2, at 29 and 32 ns, for example, correlate strongly with the O1-C1-C2-O2 dihedral angle, which in turn correlates strongly with whether HO1 is H-bonded to Glu165 OE2, Ser96 OG, or to a water h-bonded to Ser96 OG, i.e., internal torsional motions within DHAP. Transient regions of the trajectory for which the closest water makes sudden increases to near 4 Å correlate well with the intrusion of the large hydrophobic side chain of Ile170, which is effectively in van der Waals contact with the *pro-R* proton during such intervals.

In addition, during the exceptional upward fluctuation in the OE distances at 16 ns, DHAP is seen to make a short separation from Glu165. The closest water at the same instant becomes much closer by virtue of an instantly constructed 3-water wire stretching from phosphate to Ser96 OG, which remains attached to Glu165 by the double H-bond backbone “grip”, which in turn allows DHAP to regain its H-bond to Glu165.

**Causes of distance fluctuations seen in Fig. 1(B) of text).** During the 200 ns run MD simulation DHAP is initially H-bonded to Glu165 OE2 via HO1 with a very short *proR*-OE2 distance and a close water, which remarkably remains trapped between OE2, Leu230 O and Gly210 for 54 ns, with another water bridging to phosphate. From 54-64.5 ns it alone bridges from OE2 to phosphate. The large spike to ~8 Å for the OE2 distance at from 7.4-10.5 ns coincides with DHAP becoming detached from Glu165 and re-attaching at 8.5 ns. During the 0-10.5 ns, Ser96 has no significant grip on Glu165. Histograms of the distances plotted in Fig. 2B are shown in Fig. S2.

**Further discussion of  $pK_a$  in the enzyme.** Further circumstantial evidence comes from the TIM enzymatic activity vs. pH study of Plaut and Knowles [9] in which maximal activity was observed between pH 6 and 8.5, and fell off steeply outside those limits. This is not consistent with the normal  $pK_a$  of glutamate in proteins, but Glu165 was considered a reasonable candidate for the titrating base, even though the  $pK_a$  for the glutamate side chain is typically given as ~4. The Plaut-Knowles pH study is ambiguous because the  $pK_a$  of Glu and Asp can be as high as 7 when buried in a protein, while the normal  $pK_a$  for DHAP is 6, entirely due to the phosphate. As noted in the text, however, the abundant access of water to Glu165 carboxylate, suggests that environment should *not* be considered “hydrophobic”. Plaut and Knowles also used the argument from Eigen[11] that all common bases, with oxygen, nitrogen or sulfur centers, combine with protons in aqueous solution with a second-order rate constant around  $10^{10} \text{ M}^{-1} \text{ s}^{-1}$ , concluding that “this requires that an enzymic acid group must dissociate with a rate of 20000  $\text{s}^{-1}$  and must have a  $pK_a < 6$ , unless proton tunneling is invoked”.

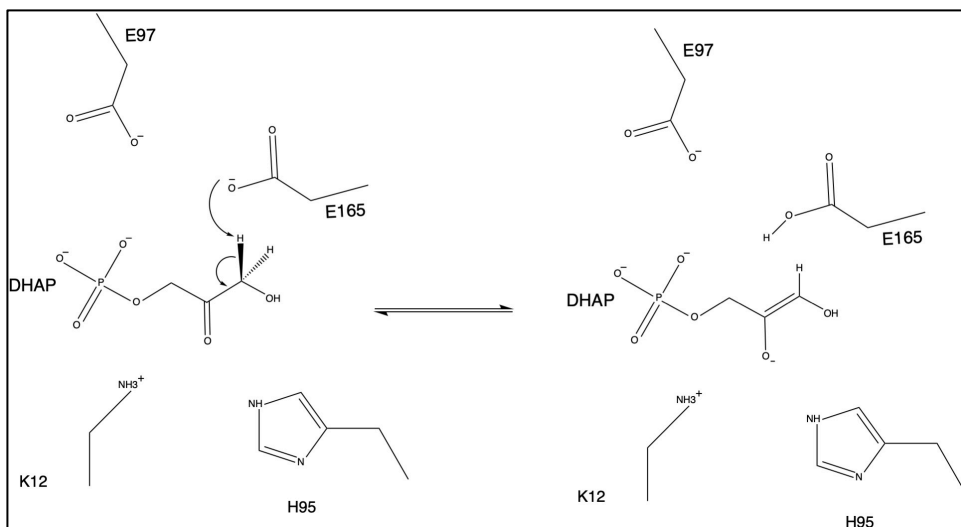


**Fig. S1.** The long-accepted mechanism of *pro-R* proton abstraction from C<sub>1</sub>. The E165 anion is the base that abstracts the proton. The other active-site members shown are *not* involved in the initial step

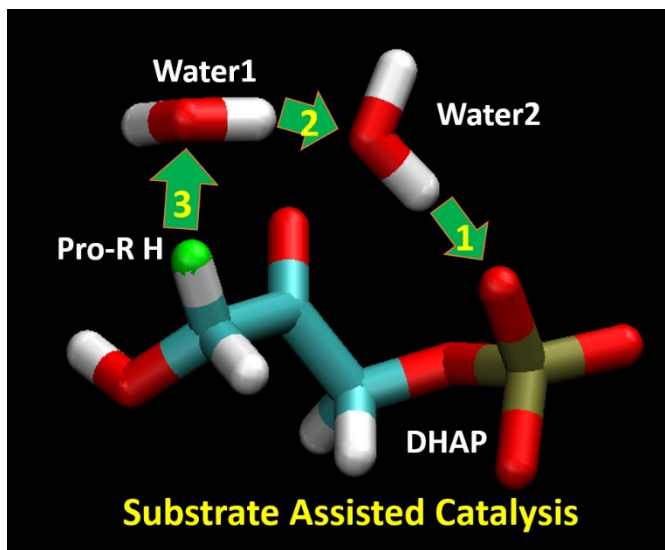


**Fig. S2.** A cartoon depicting the alternative mechanism proposed in Fig. 5 of the text, and is identical to the manuscript Table of Contents Figure.

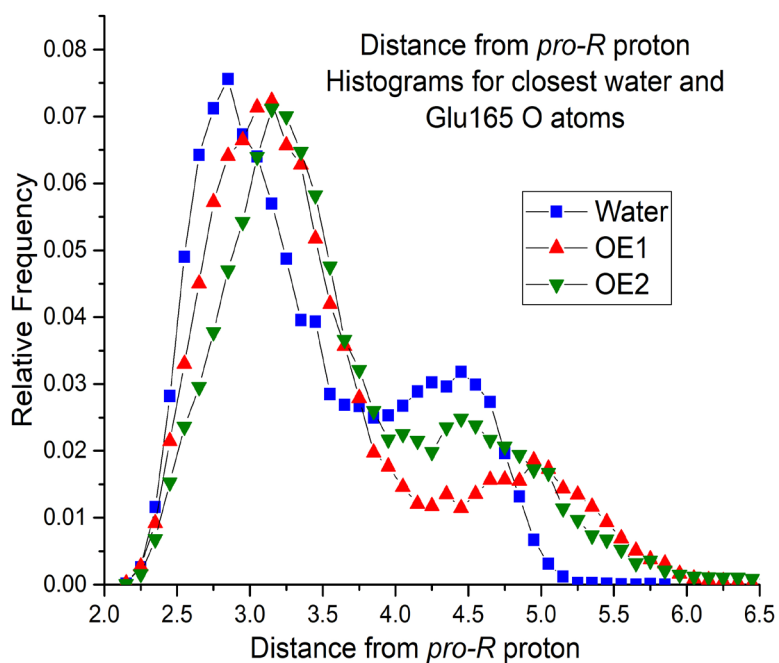


**Fig. S3.** Histograms of the distances found from the *pro-R* proton to the closest water oxygen, and to the OE oxygens of Glu165. Water in the active site is ubiquitous in MD simulations and is seen to be slightly more available for the formation of hydroxide proximal to the *pro-R* proton compared to OE distances.

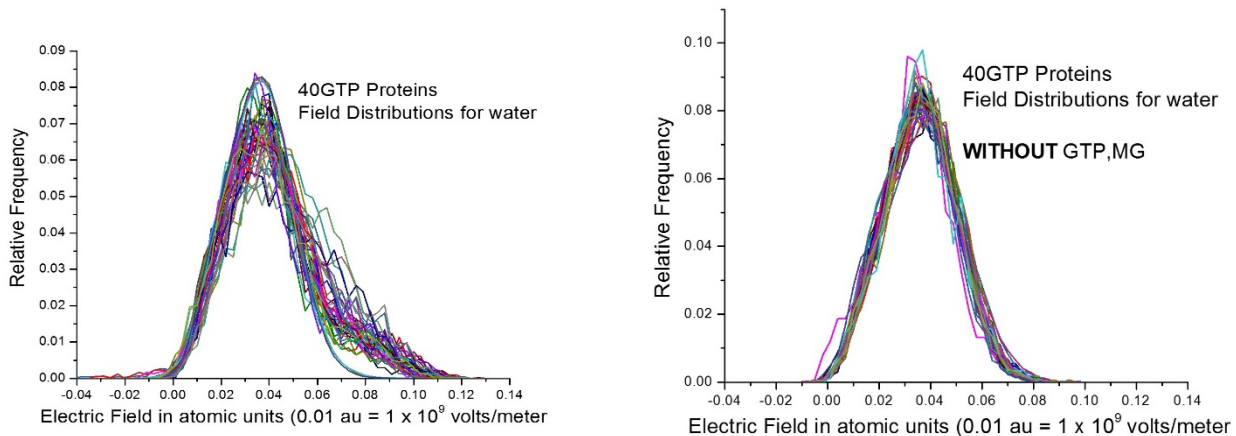


**Fig. S4.** Histograms of electric fields for **water in the active site** for 40 GTPases, **with and without GTP-Mg<sup>2+</sup>**.

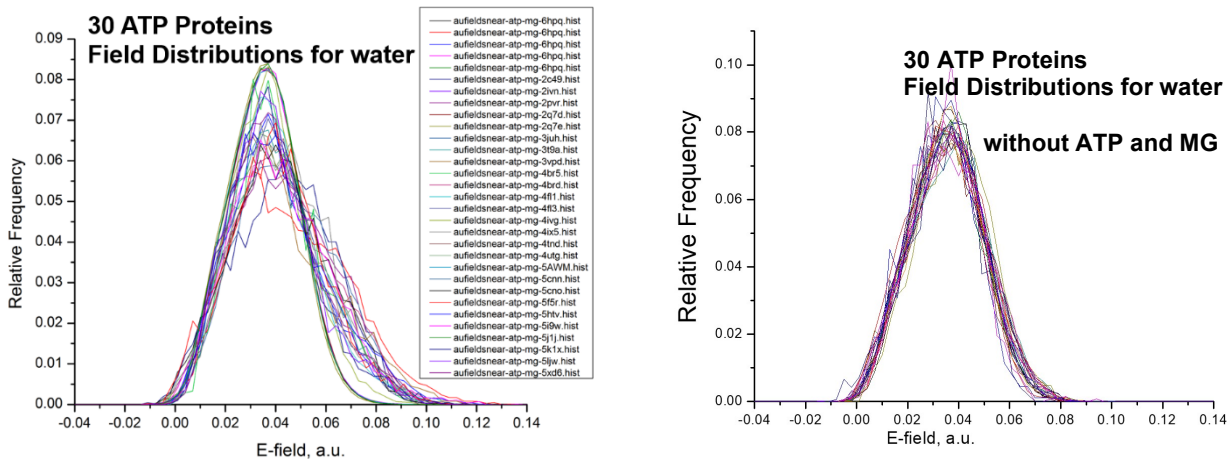


**Fig. S5.** Histograms of electric fields for **water in the active site** for 30 ATPases, **with and without ATP-Mg<sup>2+</sup>**.

**Movie S1** (separate file to be uploaded separately).

File: MovieS1-DHAP-OH.mp4 <https://chemistry.montana.edu/callis/MovieS1-DHAP-OH.mp4>

Caption: Movie of ADMP trajectory of a hydroxide ion abstracting the *pro-R* proton (atom 22) from DHAP in the presence of Glu165. Route card = # b3lyp/6-31g(d,p) admp=(maxpoints=2000,nke=37052)

## Movie S2

File: MovieS3-DimerOpt065au(12).pptx <https://chemistry.montana.edu/callis/MovieS3-DimerOpt065au.pptx>

Caption: MP4 movie of Gaussian 09 energy minimization computation of a gas phase water dimer in an applied constant electric field of 0.065 au. Route = # opt b3lyp/cc-pVTZ nosym field=x-650 scf=(xqc,maxconventionalcycles=512)

## References

1. M. J. Frisch, G. W. T., H. B. Schlegel, G. E. Scuseria, M. A. , Robb, J. R. Cheeseman, G. Scalmani, V. Barone, B. Mennucci, G. A. Petersson et al. *GAUSSIAN09* Gaussian, Inc.: 2009.
2. Iyengar, S. S.; Schlegel, H. B.; Voth, G. A.; Millam, J. M.; Scuseria, G. E.; Frisch, M. J., Ab initio molecular dynamics: Propagating the density matrix with Gaussian orbitals. IV. Formal analysis of the deviations from Born-Oppenheimer dynamics. *Israel Journal of Chemistry* **2002**, *42* (2-3), 191-202.
3. Rega, N.; Iyengar, S. S.; Voth, G. A.; Schlegel, H. B.; Vreven, T.; Frisch, M. J., Hybrid ab-initio/empirical molecular dynamics: Combining the ONIOM scheme with the atom-centered density matrix propagation (ADMP) approach. *Journal of Physical Chemistry B* **2004**, *108* (13), 4210-4220.
4. Car, R.; Parrinello, M., Unified approach for molecular-dynamics and density-functional theory. *Physical Review Letters* **1985**, *55* (22), 2471-2474.
5. M.J. Abraham, D. van der Spoel, E. Lindahl, B. Hess, and the GROMACS development team, GROMACS User Manual version 2019.5, <http://www.gromacs.org>
6. Lindorff-Larsen, K.; Piana, S.; Palmo, K.; Maragakis, P.; Klepeis, J. L.; Dror, R. O.; Shaw, D. E., Improved side-chain torsion potentials for the Amber ff99SB protein force field. *Proteins-Structure Function and Bioinformatics* **2010**, *78* (8), 1950-1958.
7. Jogl, G.; Rozovsky, S.; McDermott, A. E.; Tong, L., Optimal alignment for enzymatic proton transfer: Structure of the Michaelis complex of triosephosphate isomerase at 1.2-angstrom resolution. *Proceedings of the National Academy of Sciences of the United States of America* **2003**, *100* (1), 50-55.
8. Corcelli, S. A.; Skinner, J. L., Infrared and Raman line shapes of dilute HOD in liquid H<sub>2</sub>O and D<sub>2</sub>O from 10 to 90 degrees C. *J. Phys. Chem. A* **2005**, *109* (28), 6154-6165.
9. Corcelli, S. A.; Lawrence, C. P.; Skinner, J. L., Combined electronic structure/molecular dynamics approach for ultrafast infrared spectroscopy of dilute HOD in liquid H<sub>2</sub>O and D<sub>2</sub>O. *Journal of Chemical Physics* **2004**, *120* (17), 8107-8117.
10. Plaut, B.; Knowles, J. R., pH-Dependence of triose phosphate isomerase reaction. *Biochemical Journal* **1972**, *129* (2), 311-320
11. Eigen, M., Proton transfer acid-base catalysis + enzymatic hydrolysis .i. Elementary processes. *Angewandte Chemie-International Edition* **1964**, *3* (1), 1-19.